Research Article | Vol. 26, No. 26 | 24 Dec 2018 | OPTICS EXPRESS 34872
Optics EXPRESS

Multiple adjustable optical Tamm states in one-dimensional photonic quasicrystals with predesigned bandgaps

YUE FEI, YOUWEN LIU,* DAXING DONG, KAI GAO, SHUAI REN, AND YONGQING FAN

College of Science, Nanjing University of Aeronautics and Astronautics, Nanjing 210016, China
**ywliu@nuaa.edu.cn*

Abstract: We proposed an approach to get multiple and adjustable optical Tamm states (OTSs) by constructing a structure consisting of a metal layer and one-dimensional photonic quasicrystals with preassigned bandgaps. In the structure, multiple OTSs excited simultaneously in each bandgap were observed. We explored the physics mechanism of the multiple OTSs by analyzing the electric field intensity distribution in the structure. Besides, the results also show that the thickness of the top layer gives one more degree of freedom in designing multiple OTSs. Finally, we demonstrated that one additional OTS can be obtained independently by adding another bandgap to the proposed structure.

1. Introduction

Nowadays, photonic quasicrystals (PQCs), which were first introduced by Kohmoto [1], are an emerging substitute of photonic crystals (PCs) for its complicated spectrum. Hitherto, a plenty of works concerning PQCs have been performed [2–4]. Compared with periodic photonic crystals, PQCs exhibit more various spectrum features and better performances in applications due to their long-range order along with short-range aperiodicity. Traditional PQCs are regarded as photonic crystals consisting of alternative dielectric layers of different refractive indexes obeying substitution rules, such as Fibonacci sequence [1], Cantor sequence [5] and Thue–Morse sequence [6] etc. Recently, researchers reported a new group of PQCs described by a series of analytical expressions rather than substitution rules. This novel group of PQCs shows multiple photonic band gaps (PBGs) [7], which can be pre-designed theoretically and tuned independently by adjusting corresponding structural parameters. This versatile approach forming multiple PBGs paves a new avenue in designing optical devices.

Optical Tamm state (OTS) is a lossless optical surface state in analogy to electrical Tamm state which exists in crystal boundary in solid physics [8]. Recently, researchers investigated the OTS on the interface between a thin metal film and a traditional distributed Bragg reflector (DBR) structure [9]. It has been demonstrated that OTS can be formed either on the interface of two periodical dielectric structures with overlapped bandgaps [10] or in the boundary between a thin metal layer and a DBR structure [11]. The electric field in the structures confines at the interface between two different media and decays exponentially away from the interface in the DBR structure. More importantly, OTS can be excited both in TM and in TE polarizations, with an in-plane wave vector inside the light cone, even at normal incidence [12]. So far, extensive researches have been performed on OTS in theory [13–15] and in experiments [16–19], and many applications have been investigated in perfect absorbers [14], sensors [16], optical filters [20], and solar cells [21] for its unique spectra properties and electric field localization at the interface between metal and dielectric media. However, the deterministic structures with multiple OTSs required cannot be designed flexibly.

#347137 https://doi.org/10.1364/OE.26.034872
Journal © 2018 Received 2 Oct 2018; revised 25 Nov 2018; accepted 28 Nov 2018; published 21 Dec 2018

Optics EXPRESS

Here, we proposed a way for production of multiple and adjustable OTSs based on a thin metal film and a PQC structure. The PQC is composed of two alternative dielectric materials and the index distribution can be expressed by a superposition of several harmonics with different frequencies. The simulation results show that the number of the OTS dips can be pre-designed in theory and the locations of the OTS dips can be adjusted adequately by changing structure parameters. Therefore, this method could find potential application in spectrum engineering and integrated optics.

2. Theory model

Firstly, let us consider the PQC structure with adjustable bandgaps. The refractive index distribution along the z-axis can be depicted by an analytical expression [7]:

$$n(z) = \frac{n_A + n_B}{2} + \frac{n_A - n_B}{2}\mathrm{sgn}\left[\sum_i A_i \sin\left(\mathrm{K}_i z + \varphi_i\right)\right] \quad (1)$$

where n_A and n_B are the refractive indices of dielectric media A and B, respectively; sgn (z) = $|z|/z$ is signum function mathematically; A_i, $\boldsymbol{K}_i$ and φ_i are the amplitude, reciprocal vector (RV), and the initial phase of the i-th harmonic function, respectively. When we restrict our consideration by the case of two harmonic functions, Eq. (1) can be simplified as n(z) = (n_A + n_B)/2 + (n_A - n_B)/2 × sgn (A_1 sin ($\boldsymbol{K}_1 z + \varphi_1$) + A_2 sin ($\boldsymbol{K}_2 z + \varphi_2$)). In our numerical experiment, we assume φ_i = 0 and A_i = 1, which means each harmonic function contributes equally to the index distribution. Then $\boldsymbol{K}_i$ is the main factor that needs to be taken into account in our calculation. The central wavelengths of the bandgaps of the PQC can be given by:

$$\lambda_{m,i} = \frac{2\pi\left(n_A + n_B\right)}{mK_i} \quad (2)$$

where m is an integer representing the order of the bandgap (here we assume m = 1), i is the i-th bandgap corresponding to the i-th harmonic function.

OTSs can be generated by adding a metal layer on the top of the PQC structure [9,22]. The eigenfrequencies of OTSs must satisfy the phase matching condition [12]:

$$r_m r_{PQC} = 1 \quad (3)$$

where r_{PQC} is the reflection coefficient of the light incident from the dielectric medium to the PQC structure; r_m is the reflection coefficient of the light incident on a metal, given by Fresnel formula r_m = (n_A - n_m) / (n_A + n_m), where n_m is the refractive index of the metal. The reflection coefficient r_{PQC} can be obtained by the transfer matrix method [23]. Based on the discussion above, we can design the central frequencies of the bandgaps of the PQC by choosing $\boldsymbol{K}_i$ properly and predict the eigenfrequencies of OTSs in theory. Meanwhile, the number of OTSs excited simultaneously in respective bandgaps can be tuned flexibly by inserting different harmonic functions into the analytical expression (Eq. (1)).

3. Results and discussions

In our simulation, we mainly focus on the case of TE polarization, while similar discussions are also applied to TM polarization. We select GaAs and AlAs as the dielectric layers A and B with n_A = 3.56 and n_B = 2.95 [24], because they are usually used as typical DBR material grown by gas source molecular beam epitaxy [9,19,20]. On the top of the DBR, there is a thin gold film with a thickness of d_m = 30 nm, where the permittivity of gold in infrared region can be described by the Drude model [25]. All the proposed structures were grown on a GaAs substrate. Light is incident from the metal side of the Au-PQC structure, as indicated by the blue arrows in Figs. 1(c) and 1(d). To get two bandgaps with the central wavelengths locating at λ_1 = 1000 nm and λ_2 = 1200 nm, $\boldsymbol{K}_1$ = 40.90 μm^{-1} and $\boldsymbol{K}_2$ = 34.09 μm^{-1} can be calculated

Optics EXPRESS

from Eq. (2). The refractive index distribution of the PQC structure following the analytical expression with a total length of 5μm is depicted in the upper parts of Figs. 1(c) and 1(d). The corresponding Fourier transformation of the PQC structure is shown in the Fig. 1(a) with two peaks located at $\boldsymbol{K}_1$ and $\boldsymbol{K}_2$, respectively. In Fig. 1(b), we plot the reflectivity spectra of the PQC and the Au-PQC structures calculated by the transfer matrix method. As shown in Figs. 1(a) and 1(b), two peaks in the Fourier spectrum and the two bandgaps in the reflectivity spectrum of the PQC structure show that the bandgaps are indeed adjustable and designable. The reflectivity spectrum of the Au-PQC structure undergoes two pronounced reflection dips at 1036.8 nm (λ_{OTS1}) and 1237 nm (λ_{OTS2}), which suggests that multiple OTSs are excited simultaneously in two separated bandgaps in near infrared region. The locations of OTSs are the same as the results calculated from Eq. (3).

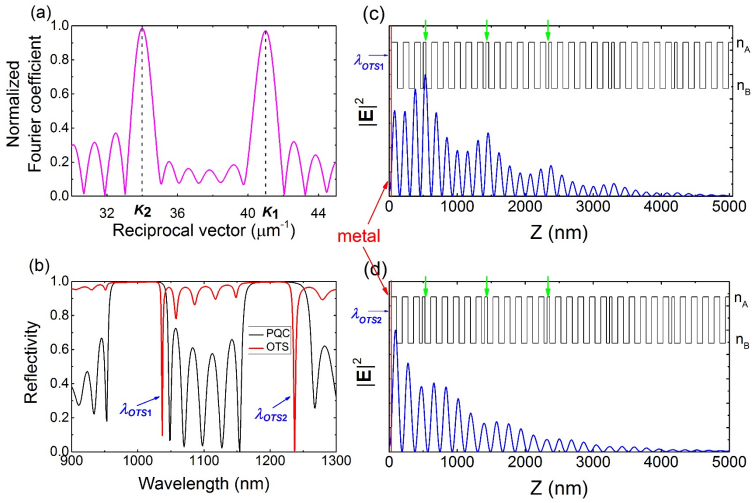

Fig. 1. (a) Fourier transformation of the index distribution of the PQC structure with $\boldsymbol{K}_1$ = 40.90 μm^{-1} and $\boldsymbol{K}_2$ = 34.09 μm^{-1}. (b) Reflectivity map of the PQC and the OTSs, and the central wavelengths of the bandgaps locate at 1000 nm and 1200 nm. Normalized electric field intensity ($|\boldsymbol{E}|^2$) of the proposed structure for (c) λ_{OTS1} = 1036.8 nm and (d) λ_{OTS2} = 1237 nm at normal incidence.

In order to explore the physics mechanism of the multiple OTSs generated in the proposed structure, the distributions of the normalized electric field intensity ($|\boldsymbol{E}|^2$) in the metal-PQC structure at the two wavelengths of λ_{OTS1} = 1036.8 nm and λ_{OTS2} = 1237 nm were simulated, which are depicted in Figs. 1(c) and 1(d), respectively. The PQC structure starts at z = 30 nm (noted by the red line) and the metal layer lies on the top of the PQC structure (in the region 0 < z < 30 nm). The difference between these two OTSs is obvious. For the case of λ_{OTS2} = 1237 nm, the electric field localizes at the interface between the metal and the dielectric layer A (GaAs) and decays exponentially along the propagation direction, as shown in Fig. 1(d). The perturbations with the minimum electrical field around z = 500 nm and z = 1400 nm noted by green arrows are due to the hetero-structure in the PQC structure, which can be referred to the refractive index distribution sketched by the upper line. However, as shown in Fig. 1(c) for the case of λ_{OTS1} = 1036.8 nm, the electric field confines at the interface of the first hetero-structure at z = 500 nm rather than the boundary of metal and dielectric layer, though the electric field intensity localized at the interface of the metal and the dielectric layer is still considerable. Meanwhile, the electric field intensity also decays exponentially along z-axis after its confinement at z = 500 nm. In fact, traditional DBR always shows monotonously exponential decay within its structure. When the defects or hetero-structures are introduced in

Optics EXPRESS

the PQC structure to obtain multiple bandgaps, the electric field perturbations with maxima or minimum at hetero-structure position arise. Thus, this phenomenon can be contributed to inherent quasiperiodic characteristics of the PQC [26].

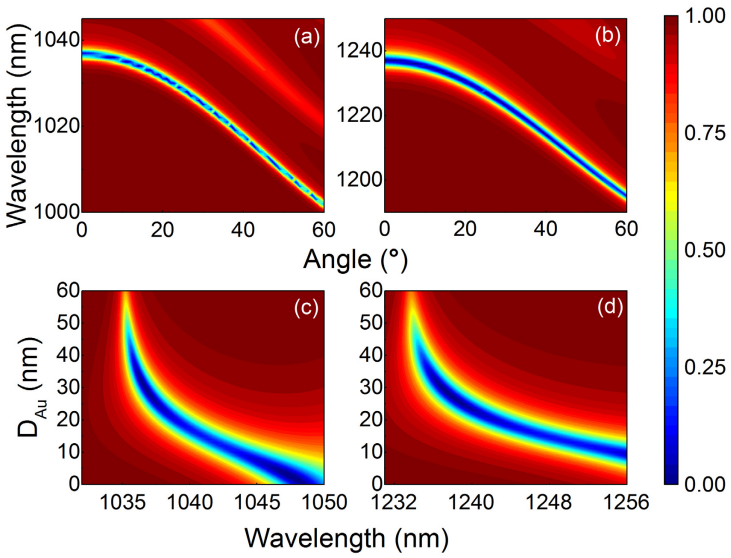

Fig. 2. Reflectivity spectra of the metal-PQC structure (Au layer thickness of 30 nm) as a function of the wavelength and the incident angle for (a) λ_{OTS1} and (b) λ_{OTS2}. Reflectivity spectra of the metal-PQC structure as a function of the wavelength and the thickness of the gold film for (c) λ_{OTS1} and (d) λ_{OTS2} at normal incidence.

To further understand the dispersion properties of the multiple OTSs in the proposed metal-PQC structure, we plot the reflectivity spectra concerning different incident angles for λ_{OTS1} and λ_{OTS2}, as shown in Figs. 2(a) and 2(b), respectively. It is evident that both OTSs generated in the bandgaps undergo a blue shift. For OTS1 generated in the first bandgap (the central wavelength of 1000 nm), λ_{OTS1} changes from 1036.8 nm to 1002 nm with increasing incident angle from 0° to 60°; while for OTS2 generated in the second bandgap (the central wavelength of 1200 nm), λ_{OTS2} changes from 1237 nm to 1195 nm with an increase of incident angle from 0° to 60°. The blue shift of the OTSs is fundamentally due to the increase of in-plane wave vector with the increment of incident angle. Furthermore, a brief research on the dispersion property of the gold layer thickness was also conducted. As shown in Figs. 2(c) and 2(d), when the metal thickness is thin enough, the increase of the metal layer thickness causes a blue shift of the wavelengths of the OTSs. When the metal thickness increases to d_m = 50 nm or more, the OTSs become weaker and disappear eventually. It is easy to understand this phenomenon. When the thickness of the gold layer exceeds the penetration depth, the metal will reflect the incident wave back and OTS will no longer exist.

Furthermore, we investigated the properties of multiple OTSs for TM polarization in the Au-PQC structure. Usually, the bandgaps become narrower for TM mode than TE mode, which is especially remarkable in large incidence angles as shown in Fig. 3(a), where the bandgaps of the PQC structure at a large angle of 80° are plotted. However, this narrower bandgap does not influence the existence of multiple OTSs. Figure 3(b) shows the wavelengths of the OTSs of the Au-PQC as a function of incidence angle for TE and TM modes. With the angle increased from 0° to 80°, both TE (solid line) and TM (dash line) OTSs undergo blue shift in the same trend. As the incident angle becomes larger, the TM OTSs shift more than TE OTSs. It is worth noting that when the structure is designed, Brewster angle has to be considered for TM polarization. To get omnidirectional photonic

Optics EXPRESS

bandgap, the maximum refraction angle must be smaller than the minimum Brewster angle inside the structure [27]. In our design, the maximum refraction angle $\theta_{Rmax} = \sin^{-1}(n_{air}/n_B) = 19.81°$ is smaller than the minimum Brewster angle $\theta_{Bmin} = \tan^{-1}(n_B/n_A) = 39.64°$, which means the incidence wave from outside cannot be coupled to Brewster's window. That is to say, the Brewster angle will not influence the existence of multiple OTSs for TM polarization.

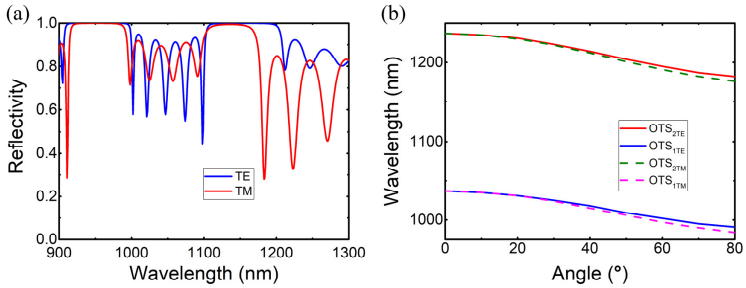

Fig. 3. (a) Bandgaps of the PQC structure for TE and TM polarizations at an incident angle of 80°. (b) OTSs of the Au-PQC structure at different incident angle for TE and TM polarizations.

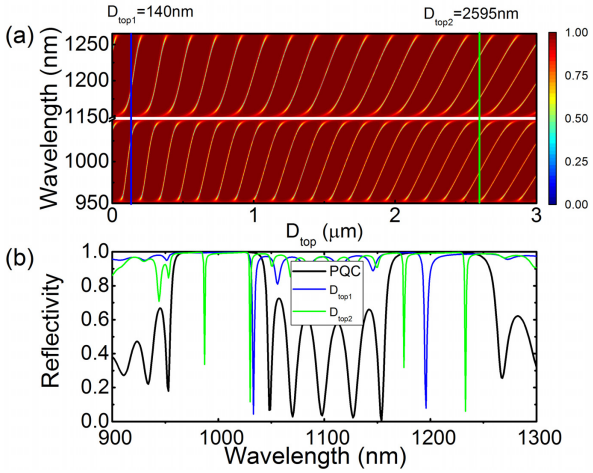

Fig. 4. (a) OTSs with respect to the incident wavelength and the thickness of the top layer. The thickness of the top layer (D_{top}) ranges from 0 to 3000 nm. The colored vertical lines indicate different D_{top}. (b) Multiple OTSs for different thickness of the top layer. The colored lines correspond to the colored vertical lines in (a).

More interestingly, we achieved periodic modification of OTSs in its respective bandgaps by increasing the thickness of the top dielectric layer A (D_{top}) in the structure. The calculated reflectivity spectra are showed in Fig. 4(a). We omitted the y axis from 1050 to 1150 nm for the convenience of observation and discussion. Apparently, the golden tilted stripes in Fig. 4(a) are non-paralleled with each other. In this case, the top layer can be considered as a Fabry-Perot cavity between the metal layer and the PQC structure, and the slope can be calculated as $d\lambda/dD_{top} \approx (2n_A)/N$ from the resonant condition of the Fabry-Perot cavity, where N is a natural number indicating the N-th strip. With the increase in thickness of the top layer, multiple OTSs may appear in each bandgap, and their wavelengths may be calculated by the resonant condition of the Fabry-Perot cavity. We can investigate this kind of multiple OTSs by adding perpendiculars representing different D_{top} in Fig. 4(a). The different vertical lines converge with the strips in one or more points, indicating single OTS or multiple OTSs

Optics EXPRESS

excited in one bandgap. In Fig. 4(b), we demonstrate the multiple OTSs with respect to the different D_{top} in Fig. 4(a), where the blue line represents D_{top1} = 140 nm and the green line represents D_{top2} = 2595 nm. As shown in Fig. 4(b), the two reflection dips λ_1 = 1033 nm and λ_2 = 1196 nm appear in two bandgaps of the PQC for D_{top1} = 140 nm; while the four reflection dips are located at λ_{11} = 987 nm, λ_{12} = 1030 nm and λ_{21} = 1175 nm, λ_{22} = 1233 nm for D_{top2} = 2595 nm, respectively. The tunable property of the OTSs in the proposed structure gives us more choices when designing devices and facilities.

We demonstrated our proposal by adding another bandgap in the reflectivity map, as shown in Fig. 5. Here, we set three bandgaps with the central wavelengths as 1000 nm, 1200 nm and 1400 nm, respectively. The corresponding $\boldsymbol{K}_i$ can be derived from Eq. (2): $\boldsymbol{K}_1$ = 40.90 μm^{-1}, $\boldsymbol{K}_2$ = 34.09 μm^{-1} and $\boldsymbol{K}_3$ = 29.22 μm^{-1}, and the distribution of refractive index of the 3-bandgap PQC structure is plotted in Fig. 5(a). As shown in Fig. 5(b), one can see that the pronounced OTS can be obtained in each bandgap, and the wavelengths of these three OTSs are located at λ_{OTS1} = 1036.8 nm, λ_{OTS2} = 1237 nm and λ_{OTS3} = 1426 nm, respectively. It means that the former two OTSs (OTS1 and OTS2) remain unchanged with another OTS in the structure. This result reveals that all the OTSs designed by the analytical expressions can be tuned independently. Additionally, it declares that our method is sufficiently accurate and indeed feasible in designing devices with multiple OTSs.

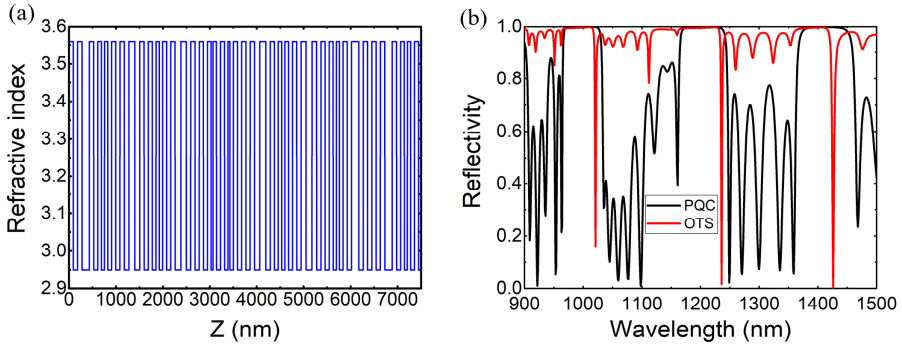

Fig. 5. A three-bandgap structure derived from Eq. (1) with $\boldsymbol{K}_1$ = 40.90 μm^{-1}, $\boldsymbol{K}_2$ = 34.09 μm^{-1} and $\boldsymbol{K}_3$ = 29.22 μm^{-1}. (a) Index distribution. (b) Three OTSs generated in the Au-PQC structure.

In fact, we may also construct PQC stacks by selecting dielectric materials such as TiO_2/SiO_2 of lower refractive index in place of GaAs/AlAs. In that case, we may obtain multiple bandgaps with the same central wavelengths only by decreasing the reciprocal vectors according to Eq. (2). The corresponding OTSs still exist in the bandgaps, and the basic properties of OTSs remain unchanged. Due to higher refractive index of GaAs and AlAs, the central wavelengths of bandgaps are more sensitive to the fabrication error. For dual-bandgap PQC, the central wavelengths of each bandgap and the wavelengths of OTSs show about 5% shift when the uniform fabrication error is 5%. Thus, the shift of OTS wavelength is about 12 nm per nanometer fabrication error for GaAs/AlAs PQC, while the value is about 6.4 nm for TiO_2/SiO_2 PQC. Therefore, the fabrication tolerance is better with lower dielectric materials.

4. Conclusion

In summary, we demonstrated multiple optical Tamm states in photonic quasicrystals with adjustable bandgaps, which can be pre-designed theoretically. The multiple OTSs can be tuned flexibly by adjusting the parameters of the proposed analytical expression. Also, we explored the dispersion relations of the incident angle and the thickness of the metal film, both of which can cause a shift on the OTSs. Furthermore, we studied the impact of the top

Optics EXPRESS

layer thickness, which introduces another variable for multiple OTSs. Finally, we verified our assumption by manifesting a three-OTS structure. The wavelengths of OTSs keep unchanged regardless of the insertion of another OTS. The proposed structure has a potential application in multichannel filter and it is a promising candidate for a precision optical comb because of its designable bandgaps and reflection dips.

Funding

Foundation of Graduate Innovation Center in Nanjing University of Aeronautics and Astronautics (NUAA) (kfjj20170802); National Natural Foundation of China (Grant No. 61675095).

References

1. M. Kohmoto, B. Sutherland, and K. Iguchi, "Localization of optics: Quasiperiodic media," Phys. Rev. Lett. **58**(23), 2436–2438 (1987).
2. Z. V. Vardeny, A. Nahata, and A. Agrawal, "Optics of photonic quasicrystals," Nat. Photonics **7**(3), 177–187 (2013).
3. E. Maciá, "Exploiting aperiodic designs in nanophotonic devices," Rep. Prog. Phys. **75**(3), 036502 (2012).
4. L. Dal Negro and S. V. Boriskina, "Deterministic aperiodic nanostructures for photonics and plasmonics applications," Laser Photonics Rev. **6**(2), 178–218 (2012).
5. S. V. Gaponenko, *Introduction to Nanophotonics* (Cambridge University, 2010).
6. L. Dal Negro, M. Stolfi, Y. Yi, J. Michel, X. Duan, L. C. Kimerling, J. LeBlanc, and J. Haavisto, "Photon band gap properties and omnidirectional reflectance in Si/SiO2 Thue-Morse quasicrystals," Appl. Phys. Lett. **84**(25), 5186–5188 (2004).
7. A. M. Vyunishev, P. S. Pankin, S. E. Svyakhovskiy, I. V. Timofeev, and S. Y. Vetrov, "Quasiperiodic one-dimensional photonic crystals with adjustable multiple photonic bandgaps," Opt. Lett. **42**(18), 3602–3605 (2017).
8. A. V. Kavokin, I. A. Shelykh, and G. Malpuech, "Lossless interface modes at the boundary between two periodic dielectric structures," Phys. Rev. B Condens. Matter Mater. Phys. **72**(23), 233102 (2005).
9. M. Kaliteevski, I. Iorsh, S. Brand, R. A. Abram, J. M. Chamberlain, A. V. Kavokin, and I. A. Shelykh, "Tamm plasmon-polaritons: possible electromagnetic states at the interface of a metal and a dielectric Bragg mirror," Phys. Rev. B Condens. Matter Mater. Phys. **76**(16), 165415 (2007).
10. A. Kavokin, I. Shelykh, and G. Malpuech, "Optical Tamm states for the fabrication of polariton lasers," Appl. Phys. Lett. **87**(26), 261105 (2005).
11. M. E. Sasin, R. P. Seisyan, M. A. Kalitteevski, S. Brand, R. A. Abram, J. M. Chamberlain, A. Y. Egorov, A. P. Vasil'ev, V. S. Mikhrin, and A. V. Kavokin, "Tamm plasmon polaritons: slow and spatially compact light," Appl. Phys. Lett. **92**(25), 251112 (2008).
12. I. A. Shelykh, M. Kaliteevskii, A. V. Kavokin, S. Brand, R. A. Abram, J. M. Chamberlain, and G. Malpuech, "Interface photonic states at the boundary between a metal and a dielectric Bragg mirror," Phys. Status Solidi., A Appl. Mater. Sci. **204**(2), 522–525 (2007).
13. S. Brand, M. A. Kaliteevski, and R. A. Abram, "Optical Tamm states above the bulk plasma frequency at a Bragg stack/metal interface," Phys. Rev. B Condens. Matter Mater. Phys. **79**(8), 085416 (2009).
14. Y. Gong, X. Liu, L. Wang, H. Lu, and G. Wang, "Multiple responses of TPP-assisted near-perfect absorption in metal/Fibonacci quasiperiodic photonic crystal," Opt. Express **19**(10), 9759–9769 (2011).
15. G. Zheng, M. Qiu, F. Xian, Y. Chen, L. Xu, and J. Wang, "Multiple visible optical Tamm states supported by graphene-coated distributed Bragg reflectors," Appl. Phys. Express **10**(9), 092202 (2017).
16. Y. Tsurimaki, J. K. Tong, V. N. Boriskin, A. Semenov, M. I. Ayzatsky, Y. P. Machekhin, G. Chen, and S. V. Boriskina, "Topological engineering of interfacial optical Tamm states for highly sensitive near-singular-phase optical detection," ACS Photonics **5**(3), 929–938 (2018).
17. N. Li, T. Tang, J. Li, L. Luo, P. Sun, and J. Yao, ""Highly sensitive sensors of fluid detection based on magneto-optical optical Tamm state," Sensor. Actuat B **265**, 644–651 (2018).
18. M. A. Kaliteevski, A. A. Lazarenko, N. D. Il'inskaya, Y. M. Zadiranov, M. E. Sasin, D. Zaitsev, V. A. Mazlin, P. N. Brunkov, S. I. Pavlov, and A. Y. Egorov, "Experimental demonstration of reduced light absorption by intracavity metallic layers in Tamm plasmon-based microcavity," Plasmonics **10**(2), 281–284 (2015).
19. M. Wurdack, N. Lundt, M. Klaas, V. Baumann, A. V. Kavokin, S. Höfling, and C. Schneider, "Observation of hybrid Tamm-plasmon exciton- polaritons with GaAs quantum wells and a $MoSe_2$ monolayer," Nat. Commun. **8**(1), 259–264 (2017).
20. H. Zhou, G. Yang, K. Wang, H. Long, and P. Lu, "Multiple optical Tamm states at a metal-dielectric mirror interface," Opt. Lett. **35**(24), 4112–4114 (2010).
21. X.-L. Zhang, J.-F. Song, J. Feng, and H.-B. Sun, "Spectral engineering by flexible tunings of optical Tamm states and Fabry-Perot cavity resonance," Opt. Lett. **38**(21), 4382–4385 (2013).
22. M. K. Shukla and R. Das, "Tamm-plasmon polaritons in one-dimensional photonic quasi-crystals," Opt. Lett. **43**(3), 362–365 (2018).

Optics EXPRESS

23. M. Born and E. Wolf, *Principles of Optics* (Cambridge University, 1999).
24. S. Gehrsitz, F. K. Reinhart, C. Gourgon, N. Herres, A. Vonlanthen, and H. Sigg, "The refractive index of AlxGa1−xAs below the band gap: accurate determination and empirical modeling," J. Appl. Phys. **87**(11), 7825–7837 (2000).
25. N. Liu, M. Mesch, T. Weiss, M. Hentschel, and H. Giessen, "Infrared perfect absorber and its application as plasmonic sensor," Nano Lett. **10**(7), 2342–2348 (2010).
26. S. S.-U. Rahman, T. Klein, S. Klembt, J. Gutowski, D. Hommel, and K. Sebald, "Observation of a hybrid state of Tamm plasmons and microcavity exciton polaritons," Sci. Rep. **6**(1), 34392 (2016).
27. H.-Y. Lee and T. Yao, "Design and evaluation of omnidirectional one-dimensional photonic crystals," J. Appl. Phys. **93**(2), 819–830 (2003).